Li *et al. Chem. Biol. Technol. Agric.* (2024) 11:62
https://doi.org/10.1186/s40538-024-00590-0

Chemical and Biological Technologies in Agriculture

RESEARCH

Open Access

An increased wax load on the leaves of goji plants (*Lycium barbarum*) results in increased resistance to powdery mildew

Jie Li[1,2*], Xia Wen[3], Sheng-dong Zhang[1], Xiao Zhang[1], Li-dan Feng[4] and Jing He[1,2]

Abstract

Background Goji (*Lycium barbarum*) is an important economic crop that is widely cultivated in Northwest China and is known as superfood. Goji plants are often affected by powdery mildew (*Arthrocladiella mougeotii*) in the field, resulting in considerable reduction in production and serious economic losses. The long-term reliance on agricultural chemicals to control powdery mildew not only leads to environmental pollution, but also causes excessive residues to accumulate in fruits, endangering human health. The plant epicuticular wax is the first physical barrier between land plants and the atmospheric environment, and plays an important role in the interactions of plants with pathogenic microorganisms. However, the relationship between epicuticular wax and powdery mildew resistance in goji plants is not well understood.

Results The leaf epicuticular wax crystals of 'Ningqi I' goji were dense and small, and the wax load was 121.74 μg/cm^2, which was 3.36 times greater than that of 'Huangguo' goji. The ratio of alcohol components in 'Ningqi I' goji was 121.18% greater than that in 'Huangguo' goji. The incidence rate and disease index of 'Ningqi I' goji inoculated with powdery mildew were significantly lower than those inoculated 'Huangguo' goji, showing high resistance and moderate susceptibility, respectively. After mechanical wax removal, the disease indices of the two goji varieties increased significantly, indicating extreme susceptibility. Seventeen differential expression genes showing significantly greater expression in 'Ningqi' goji leaves than in 'Huangguo' goji leaves were enriched in genes involved in fatty acid elongation and the wax biosynthesis pathway. The FAR activity and relative expression levels of *LbaFAR* and *LbaWSD1* in 'Ningqi I' goji were significantly greater than those in 'Huangguo' goji. The relative expression levels of these genes significantly increased in the overexpression tobacco lines FAR-OE and WSD1-OE, and the wax load were augmented by 46.10% and 22.23%, respectively.

Conclusions The increased expression of the *LbaFAR* and *LbaWSD1* genes in 'Ningqi I' leaves led to increased FAR and WSD1 activity, increasing the wax load and alcohol content of the epicuticular of leaves, and improving leaf glossiness, resulting in strengthened resistance to powdery mildew. Therefore, the production of leaf epicuticular wax mediated by the *LbaFAR* and *LbaWSD1* genes could be the main reason for the difference in powdery mildew resistance between the two goji varieties, which can provide a theoretical basis for the selection of resistant varieties to control goji powdery mildew.

Keywords Goji, Leaf epidermis wax, Wax biosynthesis pathway, Powdery mildew, Disease resistance

*Correspondence:
Jie Li
lj81658@gsau.edu.cn
Full list of author information is available at the end of the article

Graphical Abstract

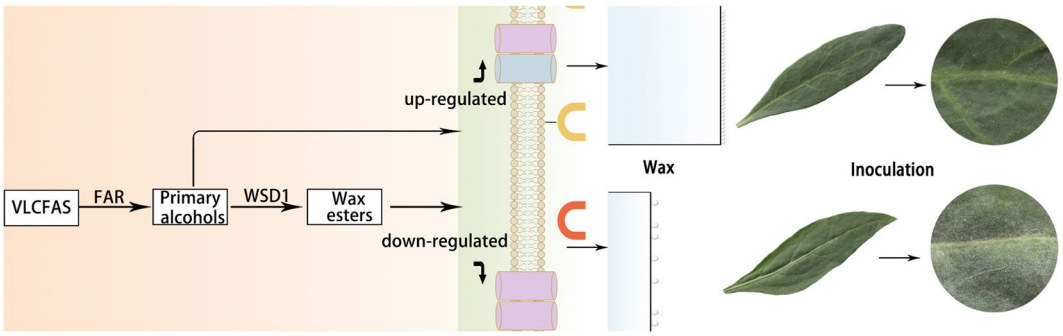

Background

Plant epicuticular wax is a hydrophobic layer that covers the surface of all terrestrial plant epicuticular cells, contributing to plant adaptation to the terrestrial environments by acting in plants as a physical barrier [1]. Studies have shown that, epicuticular wax has important functions, such as resisting UV damage [2], maintaining plant surface cleanliness [3], resisting pest and disease invasion [4] and preventing nonstomatal water evaporation [5]. The load and composition of plant wax are regulated by plant species, developmental stages, and organs [6] as well as by the environment [7]. The load, crystal structure, and components of plant wax substantially impact the occurrence of infectious diseases [8]. Epicuticular wax not only affects the adhesion and colonization of microorganisms [9], but its components and special carbon chain lengths may also act as signaling substances for plant resistance to pathogens [10, 11]. Mutations in *SHINE* transcription factors related to *Arabidopsis* cuticle wax induce defects in the stratum corneum and ultimately susceptibility to grey mould (*Botrytis cinerea*) [12]. The cuticle wax of maize (*Zea mays*) silk plays a positive role resistance to *Fusarium verticillioides* infection [13]. Sorghum (*Sorghum bicolor*) increases the resistance to anthracnose (*Colletotrichum graminicola*) by affecting the physiological and transcriptomic responses of epithelial wax [14].

Goji (*Lycium barbarum*) berries, which are considered as a superfood by consumers [15, 16] with high economic value, are mainly cultivated in Northwest China. However, during the cultivation of goji berries, they are susceptible to invasion by pests and diseases. Powdery mildew (*Arthrocladiella mougeotii*) is an extremely serious disease of goji plants, that mainly harms new shoots and leaves, causing the affected leaves to shrink, curl, and deform, which severely affects leaf photosynthesis and thus leads to decrease in yield [17]. In September 2014, powdery mildew occurred in ~ 70% of goji fields around Wuzhong city, Ningxia Province [18]. Powdery mildew not only occurs in Ningxia, but also rapidly spreads in production areas such as Gansu, Qinghai, and Xinjiang, seriously affecting the development of goji industry [19]. Currently, goji powdery mildew mainly controlled by agricultural chemicals [20], which pose hidden dangers to food safety [21].

At present, research on goji has focused on the medical application of its fruit [22], and research on wax and disease resistance has been limited. Wang found that *CER1*, *CER6*, *LACS1* and other genes in goji were related to wax synthesis [23], while Li showed that *F. solani* was strongly pathogenic for goji root rot [24]. However, there are no reports on the screening and validation of wax synthesis genes, or correlations between wax and powdery mildew in goji. During the long-term cultivation process, we found that the leaves of 'Ningqi I' goji plants were smooth and possessed a silverly white lustre, while the leaves of 'Huangguo' goji plants were rough and yellow green and had no silvery white lustre. Are these phenotypes caused by differences in leaf wax load and composition? What genes regulate this process? What is the relationship between wax and powdery mildew? The answers to these inquiries have not yet been confirmed.

Therefore, in this study 'Ningqi I' and 'Huangguo' goji plants were used as experimental materials. First, we observed the leaf structure through paraffin sections, measured the wax load, and observed the differences in crystal morphology and density by scanning electron microscopy (SEM). Then, the two goji varieties were inoculated with powdery mildew to observe the disease incidence to analyze the mechanism by which wax synthesis genes regulate wax load and mediate the resistance of goji to powdery mildew. The key differentially expressed genes (DEGs) involved in fatty acid biosynthesis and wax biosynthesis were identified through

high-throughput transcriptome sequencing, the expression levels of coding genes were determined by RT–qPCR, and the activity levels of enzymes were measured by enzyme-linked immunosorbent assay (ELISA). Finally, the selected genes were subsequently transformed into *Nicotiana benthamiana*, after which the expression levels and wax loads on the leaves of the overexpression lines were determined. The results could provide a theoretical basis for controlling goji powdery mildew and breeding disease-resistant varieties.

Methods

Plant material

Ten-years-old 'Ningqi I' and 'Huangguo' goji plants were cultivated in fields under the same conditions with pruning, water and fertilizer management and pest control. Fungicide use was suspended throughout the year of the experiment.

Leaf structure analysis

Mature leaves were cut to 0.5 cm^2 with the middle of the leaves as samples, fixed with formaldehyde-acetic acid–ethanol (FAA) solution, dehydrated and dried with gradient of ethanol solutions, embedded in paraffin, and sectioned at a thickness of 12 μm [25]. Images were taken with an Olympus BX51 optical microscope, and the thicknesses of the leaves, upper and lower epidermis, palisade tissue, and sponge tissue were measured with a micrometre. The process for each sample was repeated six times.

Leaf cuticular wax load and component analysis

The mature leaves were selected as materials, the wax load was determined by the chloroform method [26], the wax-extracted leaves were scanned, the area was calculated by Image J software, and the wax load was expressed as μg/cm^2. Each sample analysis was repeated three times.

The wax components were determined according to the methods described by Chu et al. [27]. The samples for which the wax load was measured transferred to a GC bottle, 20 μL of C24 was added as an internal reference, the samples were air-dried in a fume hood, and pyridine and BSTFA were added to the GC bottle at a volume ratio of 1:1. The samples were reacted for 30 min at a constant temperature of 70 °C, quickly dried with a Termovap sample concentrator, dissolved in chloroform and allowed to reach volume. The wax components were identified by gas spectrometry-mass spectrometry (GC/MS-QP2010, Shimadzu, Japan). The GC capillary column was 12 m long and 0.2 mm in diameter. The carrier gas was nitrogen. The FID detector (Clarus 680, PE, USA) conditions were as follows: The temperature of the column membrane and FID detector was 300 ℃ and 320 ℃, respectively; the initial temperature was 80 °C, the temperature was increased to 260 ℃ at a rate of 15 ℃/min, and the temperature was maintained for10 min. Then, the temperature was increased to 320 ℃ at 5 ℃ per minute for 15 min. Wax quantification was based on the FID peaks. Each sample analysis was repeated three times.

Leaf cuticular wax crystallization patterns

The leaf cuticular wax crystallization patterns were imaged by SEM. The leaves were stored overnight in a 5% glutaraldehyde fixation solution at 4 ℃ and then transferred to a supercritical dryer for to dehydrate for more than 4 h [28, 29]. The dried samples were coated with gold for 2 min in a sputter coater (MC1000, Hitachi, Japan) and observed via SEM (S3400N, Hitachi, Japan). The leaf samples were placed facing up and subjected to SEM, at an accelerating voltage of 5 kV, after which the leaves were observed, and photos were taken with six replicates.

Powdery mildew resistance test

Samples of the pathogen (*Arthrocladiella mougeotii*) [18] were collected from the leaves of goji plants during the peak disease period, and uniformly inoculated onto the leaves via the spore shaking method. Three plants of each variety were inoculated.

Investigation and statistics of diseases

The lesion area of the leaves was investigated beginning at 10 days after inoculation (start date). Leaves were selected from each tree in the east, west, south, north, and central directions. The designated leaves were scanned to determine lesion area every 10 days until powdery mildew spread and covered the entire leaf (end date). The ratio of lesion area to total leaf area was calculated by Image J software. Three plants of each variety were surveyed.

The incidence rate and disease index were investigated at the end date. Five directions were investigated for each tree, every direction was investigated for two new shoots, and 10–15 mature leaves each shoot from top to bottom, and three plants of each variety were investigated. The incidence rate was calculated according to Eq. (1), the disease index was calculated according to Eq. (2), the disease grade was calculated according to the method of Tian Libo et al. [30] (Additional file 1: Table S4), and the disease resistance index was calculated according to the disease index (DI) of Jing et al. [31] (Additional file 1: Table S5).

$$\text{Incidence rate (\%)} = \text{Number of diseased leaves/total number of surveyed leaves} \times 100\%. \quad (1)$$

$$\text{Disease index (DI)} = \sum \frac{\left(\text{Number of diseased leaves one level} \times \text{Disease level}\right)}{\left(\text{Survey total number leaves} \times \text{Highest disease level}\right)} \times 100. \quad (2)$$

Mechanical wax removal and disease index testing

To verify the relationship between wax load and disease resistance, two varieties of plants exhibiting similar growth in a greenhouse were used as materials. Referring to the method of Figueiredo [32], the mechanical removal was performed using an aqueous solution of gum arabic (1.5 g/mL) evenly applied with a brush on the abaxial and adaxial leaf surfaces. The gum films were removed after drying. The wax load was determined, and plants were inoculated with powdery mildew. After 15 days, the disease spot area and the leaf number at each disease level were counted, and the disease index was calculated. Three trees of each variety were surveyed.

Transcriptome extraction, sequencing, comparison and analysis

Mature leaves with relatively consistent growth were collected and mixed into three samples (0.5 g) for RNA extraction and transcriptome sequencing. Total RNA was extracted using TRIzol reagent (Invitrogen, CA, USA) according to the manufacturer's protocol. RNA purity and quantity were evaluated using a NanoDrop 2000 spectrophotometer (Thermo Scientific, USA). RNA integrity was assessed using an Agilent 2100 Bioanalyzer (Agilent Technologies, CA, USA). Then the libraries were constructed using the VAHTS Universal V6 RNA-seq Library Prep Kit according to the manufacturer's instructions. Transcriptome sequencing and analysis were conducted by OE Biotech Co., Ltd. (Shanghai, China).

The libraries were sequenced on an Illumina NovaSeq 6000 platform, and 150 bp paired-end reads were generated. The raw reads for each sample were obtained. Raw reads in fastq format were first processed using fastp 1 and the low-quality reads were removed to obtain the clean reads. Then the clean reads for each sample were retained for subsequent analyses. The clean reads were mapped to the reference genome of *L. barbarum* shared by Professor Zhong-jian Liu from Fujian A&F University (https://figshare.com/articles/dataset/Wolfberry_genomes_and_the_evolution_of_Lycium_Solanaceae_/20416593) using HISAT2 [33]. The FPKM [34] of each gene was calculated and the read counts of each gene were obtained via HTSeq-count [35]. PCA analysis was performed using R (v 3.2.0) to evaluate the biological duplication of samples. Differential expression analysis was performed using the DESeq2 [36]. A Q value < 0.05 and |log2FoldChange| > 1 were set as the thresholds for significant DEGs. GO [37] and KEGG [38] pathway enrichment analyses of DEGs were performed to identify significantly enriched terms using R (v 3.2.0). Significant enrichment was defined as $P < 0.05$ after correction.

Determination of wax synthesis enzyme activity

Mature leaves of goji were selected from the same period as those used for transcriptome sequencing (1st of August). Ten leaves were collected for each sample, with 3 replicates. The samples were rapidly frozen by liquid nitrogen and stored in a − 80 ℃ freezer for future use.

Five grams of each sample were cut into pieces, put into a mortar, ground into powder with liquid nitrogen, added 45 mL of 0.01 mol/L 4 ℃ precooled PBS (pH = 7.4) buffer, homogenized thoroughly, and centrifuged for 15 min at 5000 rpm at 4 ℃, after which the supernatant was collected for analysis. The methods described in the user manual of the ELISA kits were used to determine the activities of ACC, LACS, KCS, FAR, WSD1, and MAH1, and the relevant enzyme activities were calculated based on the standard curve.

Real-time quantitative PCR expression analysis

RNA was extracted with an RNA Extraction Kit, and then diluted to 1000 ng/μL after reverse transcription to obtain cDNA. Primers were designed in the conserved region of the gene using Primer 5.0 and Oligo 7.0 software, and were synthesized by Shanghai Bioengineering Technology Service. The gene information and primers used are shown in Additional file 1: Table S1. The two-step reaction method was used to perform RT–qPCR with a SYBR Green Pro Taq HS qPCR Kit. The reaction system was prepared on ice with 20 μL of 2 × SYBR Green Pro Taq HS Premix (10.0 μL), 1 μL each of the upstream and downstream primers (0.2 μmol/mL), 2 μL of cDNA (1000 ng/μL), and 6 μL of ddH_2O. The reaction conditions were as follows: 95 ℃ predenaturation for 15 min; 95 ℃ denaturation for 15 s, based on the Tm value of the primer annealing temperature; annealing at 58 ℃ and 60 ℃ for 20 s, and extension at 72 ℃for 20 s for a total of 45

cycles. A Light Cycler 96 SW 1.1 (Roch, Switzerland) was used for RT–qPCR. The reference gene was β-actin, and the number of repeats was $n=4$. The reaction specificity was determined according to the melting curve, and the cycle threshold (CQ) value of each sample was obtained. The relative expression level of the target gene was calculated using the $2^{-\Delta\Delta Ct}$ method [39, 40].

Functional verification of wax synthesis genes

Gene cloning and vector construction

Based on data from the goji genome sequencing database, *LbaFAR* and *LbaWSD1* were shown to have significant effects on goji wax synthesis. The leaves of *L. barbarum* weighing 0.1 g were measured, and the Trizol technique was used to extract total RNA. Reverse transcription was carried out using TaKaRa's Prime Script™ RT reagent Kit with gDNA Eraser (Perfect Real Time). CDS of sequence for these two genes was obtained from the goji gene database (https://figshare.com/articles/dataset/Wolfberry_genomes_and_the_evolution_of_Lycium_Solanaceae_/20416593), and specific primers (Additional file 1: Table S2) were designed using DNAMAN software, as well as PCR amplification was carried out. The *LbaFAR* gene PCR amplification conditions were as follows: 95 ℃ predenaturation for 2 min; 95 ℃ denaturation for 30 s, annealing at 59 ℃ for 30 s, and extension at 72 ℃ for 2 min, for 40 cycles. The *LbaWSD1* gene PCR amplification conditions: 95 ℃ predenaturation for 5 min, 95 ℃ denaturation for 30 s, annealing at 58 ℃for 42 s, extension at 72 ℃ for 2 min, for 40 cycles. The PCR products of both genes were electrophoresed on 1.5% agarose gel and recovered the target band, ligated with pMD19-T cloning vector, then transformed into *E. coli* trans-5α, which was identified and sequenced to extract the plasmid. Subsequently, homologous arms of the two genes were designed, PCR amplification was performed using the above plasmid as the template and the products were subjected to gel electrophoresis for recovery (Additional file 1: Table S3). Furthermore, the expression vector *PRI101* was double-cut with *SmaI* and *KpnI* enzymes, and the gel was cut off for recovery. Then, the two target fragments were connected by homologous recombination, transformed into *E. coli* trans-5α, and then was identified and sequenced to extract the recombinant plasmid. Finally, transformed into *Agrobacterium* LBA4404 using freeze–thaw method for genetic transformation.

Agrobacterium-mediated transformation of tobacco

The screened clone-positive strain was cultured overnight in 40 mL of LB medium supplemented with 50 mg/L rifampicin and kanamycin, and then centrifuged at 5000 rpm for 5 min and suspended with sterilized water to make OD values between 0.6 and 0.8. The tobacco leaves were then infected with the solution for 8–10 min. After that, the leaves were pre-cultured on antibiotic free medium under dark conditions for 1–2 days. At last, the leaves were transferred to tobacco differentiation medium (containing 250 mg/L cephalosporin and 30 mg/L kanamycin). When the buds grew to about 1.5 cm, they were cut and transferred to rooting medium for culture. DNA of regenerated seedlings was extracted and identified by PCR.

Statistical analysis

Statistical differences within the datasets were tested by one-way ANOVA followed by a Tukey HSD post hoc test, $P \leq 0.05$ indicated a significantly difference. The standard deviation and figures were analysed with by GraphPad Prism 9.0.5 software.

Results

Phenotypic characteristics and structures of leaves

As shown in Fig. 1A, the leaves of 'Ningqi I' goji plants were dark green and smooth, with silvery white gloss, and the leaves of 'Huangguo' goji plants were yellow–green and rough and had a faint silvery white lustre. The sizes of leaves were equivalent.

The leaf thicknesses of 'Ningqi I' and 'Huangguo' goji plants were 296.00 μm and 214.22 μm, respectively (Fig. 1B, C) ($P<0.05$). The palisade tissue of 'Ningqi I' was composed of 3–4 layers of cells, the thickness was 140 μm. 'Huangguo' goji palisade tissue was composed of 1–2 layers of cells, the thickness was 70 μm (Fig. 1E) ($P<0.05$). There was no significant difference in the thickness of the upper, parallel, or lower epidermis of the leaves between two varieties (Fig. 1D, F, G).

Leaf epicuticular wax and composition

To identify the differences in leaf gloss and tactile sensation between the two goji varieties, the wax load was determined, the wax structure of the leaf epidermis was observed via SEM, and the wax components were determined via GC/MS (Fig. 2).

The wax load of 'Huangguo' goji leaves was 36.18 μg/cm^2, and that of 'Ningqi I' goji leaves was 121.74 μg/cm^2, which was 3.36 times greater than 'Huangguo' goji leaves ($P<0.05$) (Fig. 2E). SEM revealed that the wax crystals on the 'Ningqi I' leaf epidermis were small, even and dense (Fig. 2A, B). The wax crystals on the 'Huangguo' goji leaves were rod, blocky, irregularly shaped and had a sparse and uneven distribution (Fig. 2C, D). Alkanes, alcohols, fatty acids, and esters accounted for 98.04% and 95.89% of the total wax load of 'Ningqi I' and 'Huangguo' goji, respectively, which contained the same basic

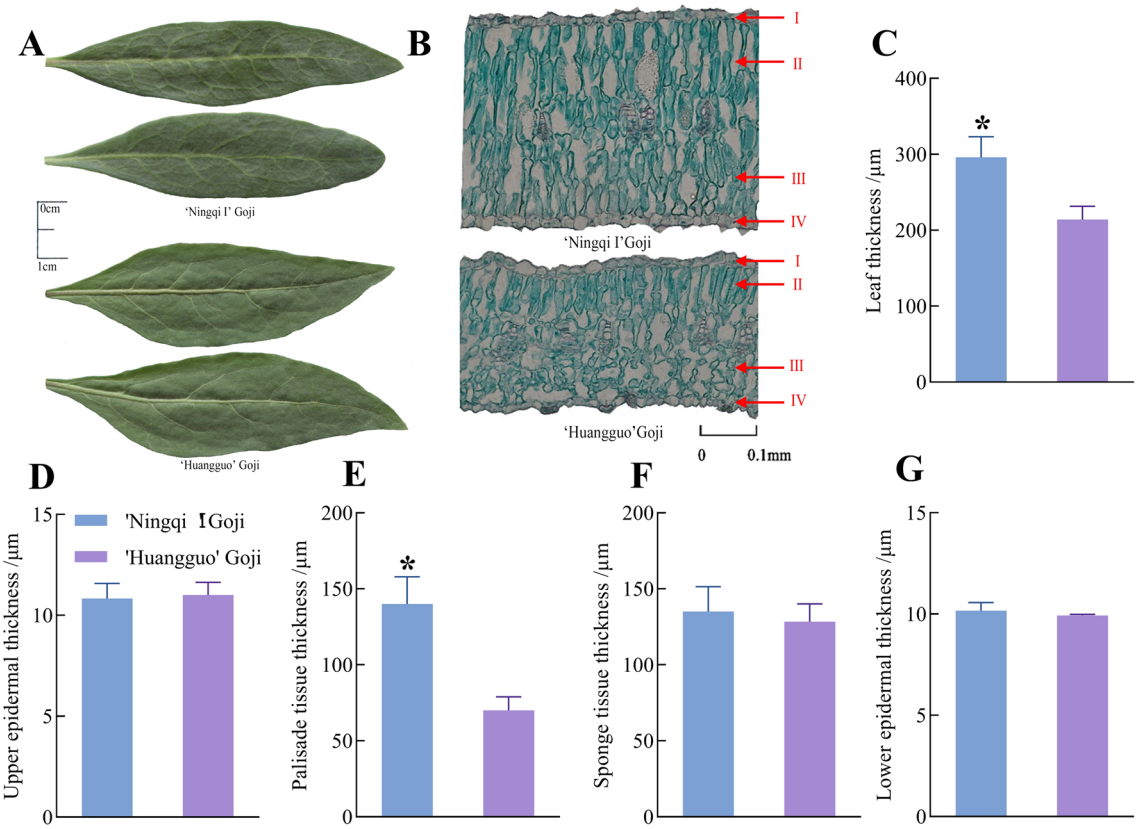

Fig. 1 The phenotypic characteristics and tissue cell structure of 'Ningqi I' goji and 'Huangguo' goji leaves. **A** Phenotypic characteristics of goji plants leaves. **B** Leaves cross–section paraffin, I Upper epicuticular, II Palisade tissue, III Sponge tissue, IV Lower epicuticular. **C** Leaf thickness. **D** Upper epicuticular thickness. **E** Palisade tissue thickness. **F** Sponge tissue thickness. **G** Lower epicuticular thickness. The '*' shown significant differences among two varieties ($P < 0.05$)

components. However, there were significant differences in the proportions of each component. The contents of alkanes and alcohols in the 'Ningqi I' leaves were 24.87% and 121.18% greater than those in 'Huangguo' goji, respectively. The contents of fatty acids and esters were 55.69% and 69.54% lower than those in 'Huangguo' goji, respectively ($P < 0.05$) (Fig. 2G).

Therefore, the differences in wax load and alcohol content might be the main reasons for differences leaf gloss and texture between the two goji varieties.

Comparison of resistance to powdery mildew between the two goji varieties

Epicuticular waxes form the outermost cuticle layer and limit the attachment of bacteria or fungi [41]. To verify the difference in disease resistance caused by wax between the two varieties, we inoculated powdery mildew on the normal leaves and leaves that underwent mechanical wax removal, the incidence and lesion area were observed, and the disease index was calculated.

As shown in Fig. 3A, B, the proportion of leaf lesion area in 'Ningqi I' was 1.66% at the start date and 4.47% at the end date, and the expansion rate was 0.14%/d. The proportion of 'Huangguo' goji leaf lesion area increased from 7.88% to 70.90%, and the expansion rate was 3.15%/d, which was significantly greater than that of 'Ningqi I'. During the observation period, the powdery mildew spot area on the 'Huangguo' goji leaf increased rapidly until it covered the whole leaf, leading to the distortion and wilting of the leaf and severe damage.

The incidence and disease indices were investigated at the end date, as shown in Fig. 3A, C, D. The incidence of in 'Ningqi I' goji was 7.85%, while the incidence of in 'Huangguo' goji was as high as 72.92%. The disease index of 'Ningqi I' goji was 1.08, indicating high resistance. The disease index of 'Huangguo' goji was as high as 24.49, indicating moderate susceptibility. Therefore, 'Ningqi I' had stronger resistance to powdery mildew.

As shown in Fig. 3E, F, G and H, after the mechanical removal of wax, there was no significant difference

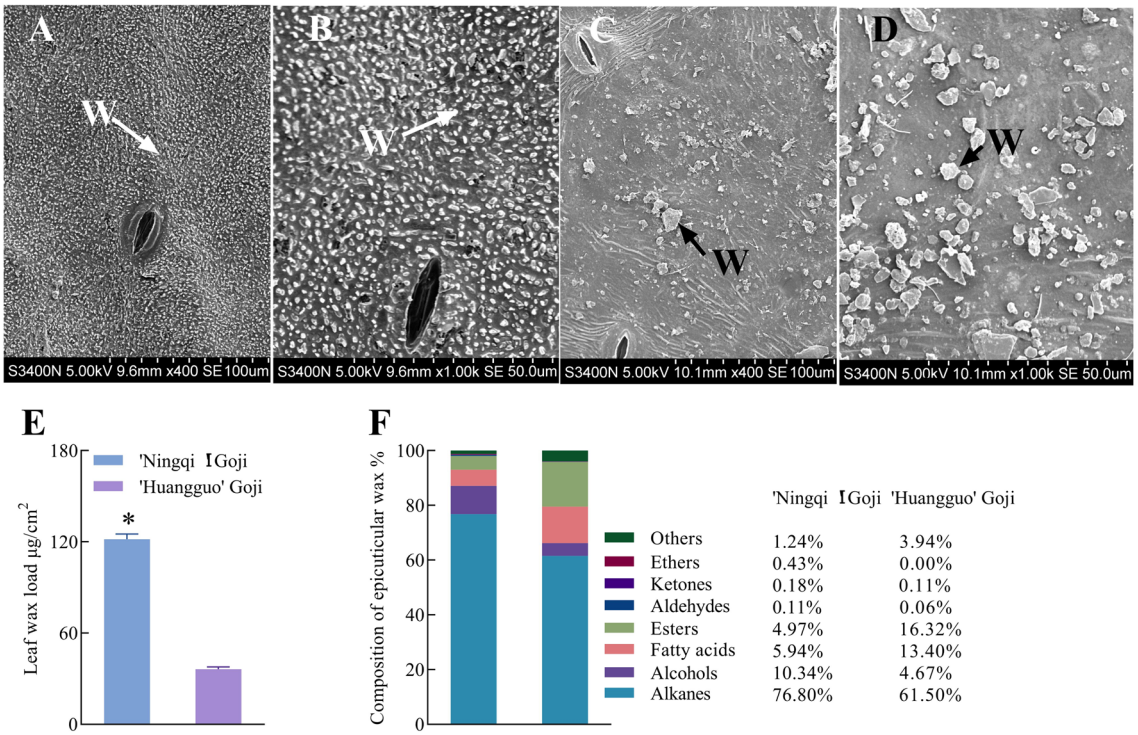

Fig. 2 The leaf wax of 'Ningqi I' and 'Huangguo' goji. **A** SEM image of 'Ningqi I' goji leaf surface at 400×. **B** SEM image of 'Ningqi I' goji leaf surface at 1000×. **C** SEM image of 'Huangguo' goji leaf surface at 400×. **D** SEM image of 'Huangguo' goji leaf surface at 1000×. **E** Leaf wax load. **F** Epicuticular wax composition. 'W' means wax crystals. The '*' shown significant differences among two varieties ($P < 0.05$)

in the epicuticular wax load between the two varieties, but the wax load decreased significantly compared to that of normal leaves (Fig. 3F). The lesion area and disease index increased significantly compared to those of normal leaves, but there was no significant difference between the two varieties, that showed extreme susceptibility to powdery mildew (Fig. 3G, H).

These results indicate that leaf epicuticular wax is a key factor in the resistance of two goji varieties to powdery mildew.

Transcriptome sequencing quality and differentially expressed genes

To analyze the differences in wax biosynthesis and alcohol-forming pathways between the two varieties, we conducted transcriptome sequencing and analysis. As shown in Additional file 1: Table S6, low-quality sequences were removed, 288.31 Mb clean reads and 41.18 Gb clean bases were obtained, and the number of clean bases in each sample reached 6.68 Gb or greater. The Q30 ranged from 95.06% to 95.27%, and the ratio of guanine to cytosine ranged from 43.14% to 44.01%. The results indicated reliable data quality.

PCA was performed on the sequencing data (Additional file 1: Fig. S1A). Principal component 1 accounted for 85.51% of the total variance, and principal component 2 accounted for 9.25% of the total variance. The 'Ningqi I' and 'Huangguo' goji samples exhibited obvious aggregation, good repeatability, and reliable sequencing data. Differential expression analysis of 'Ningqi I' and 'Huangguo' goji revealed 2511 upregulated and 3072 downregulated genes, for a total of 5583 DEGs, among which 4198 DEGs were effectively annotated, as shown as by a volcano plot (Additional file 1: Fig. S1B).

GO and KEGG enrichment analysis of transcriptome data

GO and KEGG enrichment analyses were performed on 4198 DEGs annotated by transcriptome sequencing. The GO enrichment results showed that the DEGs were mainly enriched in the tRNA metabolic process and RNA 3′-end processing of biological process, the lysosome and integral component of membrane of cellular component, and the endonuclease activity and carbohydrate binding of molecular function (Additional file 1: Fig. S2). The KEGG enrichment results showed that the DEGs were significantly enriched in three pathways: carbohydrate metabolism, signal transduction and lipid metabolism (Additional file 1: Fig. S3). GO enrichment analysis revealed that integral membrane components and KEGG

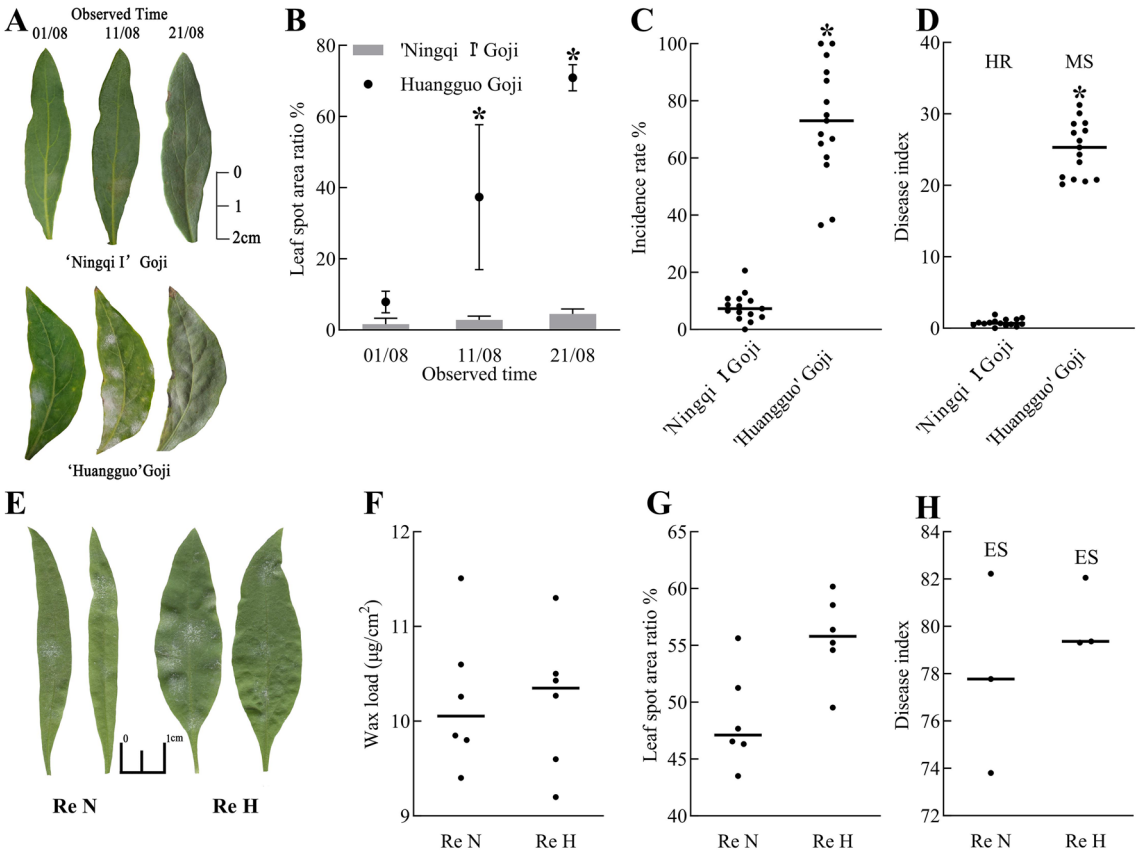

Fig. 3 The disease resistance between 'Ningqi I' goji and 'Huangguo' goji. **A** Incidence of leaf. **B** Leaf spot area ratio. **C** Incidence rate. **D** Disease index. **E** Incidence of mechanical wax removing leaf. **F** Wax load of mechanical wax removing leaf. **G** Leaf spot area ratio of mechanical wax removing leaf. **H** Disease index of mechanical wax removing leaf. Re N is mechanical wax removal of 'Ningqi I' goji; Re H is mechanical wax removal of 'Huangguo' goji; HR is high resistance. MS is moderate susceptibility. ES is extremely susceptibility '*' shows significant differences among two varieties ($P < 0.05$)

enrichment analysis revealed that lipid metabolism is closely related to plant epicuticular wax synthesis [42].

Wax metabolism pathway and gene screening

To explore the molecular mechanism of wax synthesis in goji leaves, DEGs related to fatty acid biosynthesis (GO: 0006633) and wax biosynthesis (GO: 0010025) were screened, and heatmaps were drawn based on expression levels determined via on transcriptome data and enrichment analysis results (Fig. 4).

As shown in Fig. 4, 47 DEGs were enriched in the fatty acid biosynthesis pathway, and the expression levels of five DEGs were significantly greater in 'Ningqi I' than in 'Huangguo' goji. These genes included one de novo fatty acid synthesis enzyme, acetyl-CoA carboxylase (ACC), which is encoded by the gene Lba06g02066; one ultralong chain saturated fatty acid synthesis long chain acyl-CoA synthase (LACS), which is encoded by the gene Lba06g03261; and three ultralong chain saturated fatty acid synthesis enzymes, β-ketoacyl CoA synthase (KCS), which are encoded by the genes Lba01g00543, Lba04g01329, and Lba05g02485.

Twenty-three DEGs were enriched in cutin and wax biosynthesis pathway, and the expression levels of 12 DEGs were significantly greater in 'Ningqi I' than in 'Huangguo' goji. These genes included one gene encoding aldehyde decarbonylase (AD) in the alkane synthesis pathway (Lba09g01421); four genes encoding medium chain alkane hydroxylase (MAH1) (Lba10g01984, Lba08g01893, Lba10g01985, and Lba10g01990); one gene encoding fatty acyl-reductases (FAR) in the alcohol synthesis pathway, (Lba11g02102); and six genes encoding wax ester synthase (WSD1) (Lba05g01733, Lba05g01728, Lba06g01907, Lba06g01910, Lba09g00988, and Lba05g01729).

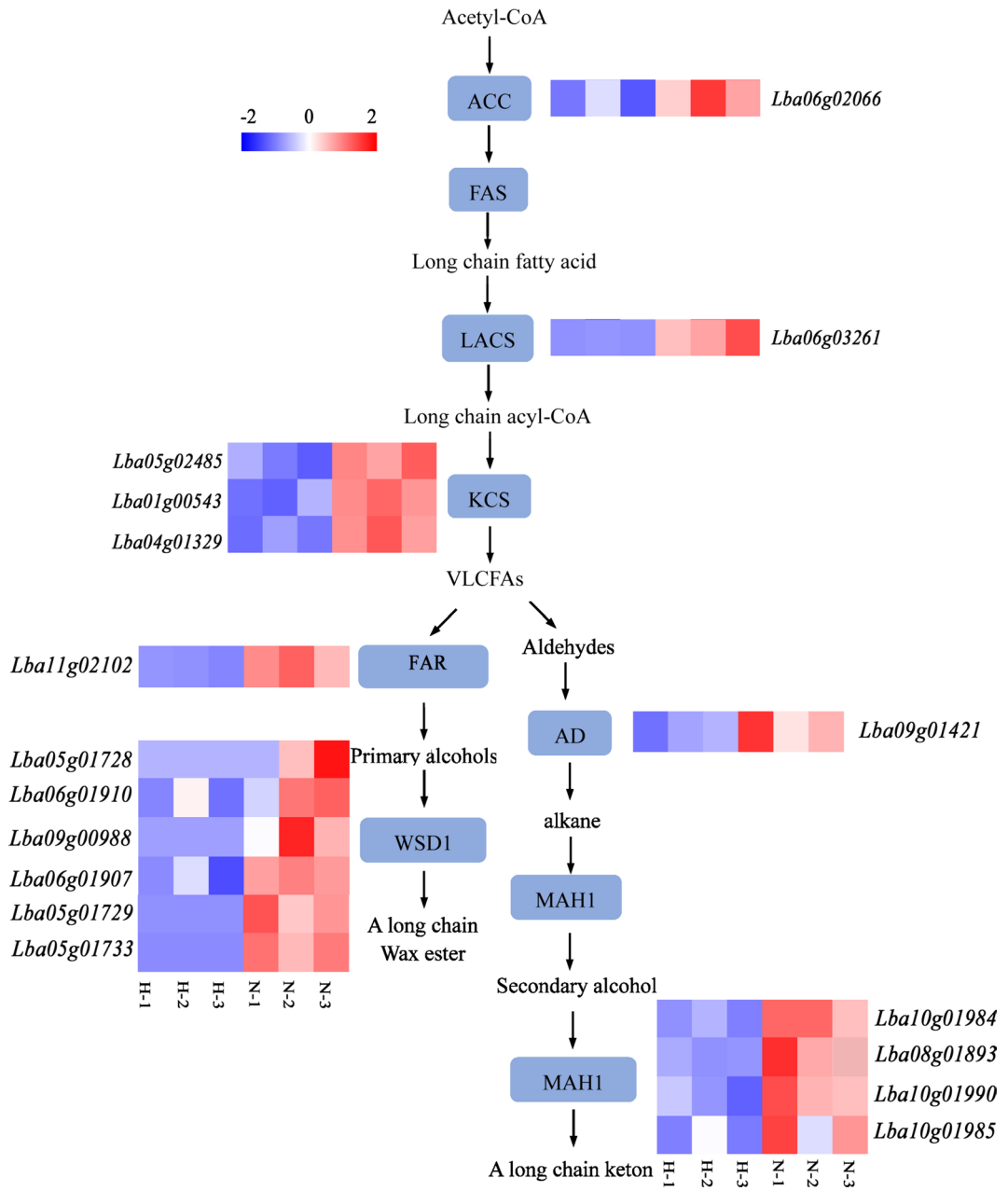

Fig. 4 Heat map of wax biosynthesis pathway and gene expression

The activities of wax synthesis enzymes and the relative expression levels of their coding genes

Based on comprehensive transcriptomic data, the expression levels of six DEGs, Lba06g02066 (*LbaACC*), Lba06g03261 (*LbaLACS*), Lba04g01329 (*LbaKCS*), Lba11g02102 (*LbaFAR*), Lba05g01733 (*LbaWSD1*) and Lba10g01984 (*LbaMAH1*), in 'Ningqi I' goji were significantly greater than those in 'Huangguo' goji. Therefore, ELISA was used to determine the corresponding enzyme activities, and RT–qPCR was used to verify the relative expression levels of the six DEGs.

As shown in Fig. 5, the activities of six enzymes and the relative expression levels of genes related to wax synthesis in 'Ningqi I' goji were significantly higher than those in 'Huangguo' goji. The FAR enzyme activity and *LbaFAR* gene relative expression were 57.29 U/L and 5.23, respectively, which were significantly greater than those of the other enzymes and genes. *LbaFAR*

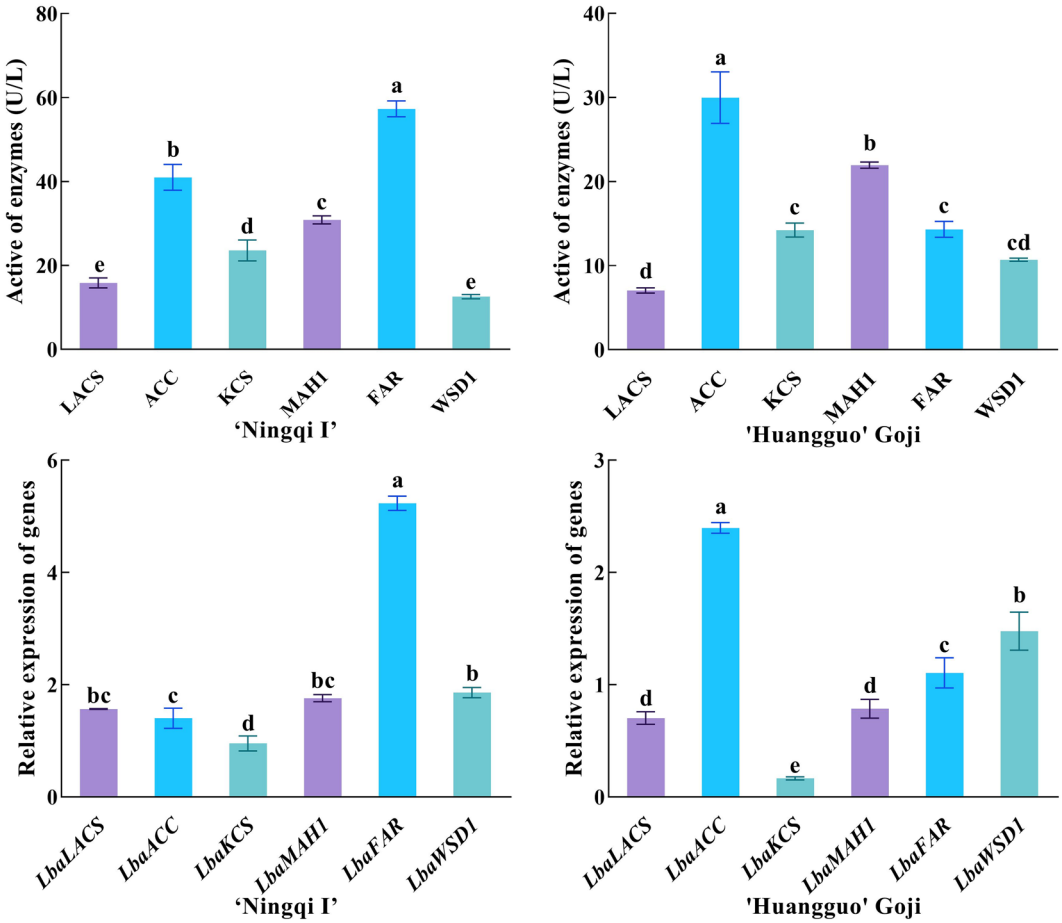

Fig. 5 Wax synthase activities and relative expression levels of coding genes. Different letters on the column indicate significant differences, while the same letter indicates insignificant differences ($P < 0.05$)

was the preferred gene for functional validation. The relative expression level of the *LbaWSD1* gene was second only to that of *LbaFAR*, reaching 1.88, so it was selected as a secondary validation gene.

VLCFAs are precursors of wax biosynthesis that are synthesized by the fatty acid biosynthesis pathway and involve multiple long metabolic pathways. The high expression of fatty acid biosynthesis pathway genes does not necessarily lead to a high epicuticular wax load. In this study, the activity of the ACC enzyme and relative expression level of *LbaACC* gene were significantly greater than those of the other genes in 'Huangguo' goji, but the epicuticular wax load was low (Fig. 2D, E). Therefore, the functions of the *LbaLACS*, *LbaACC*, and *LbaKCS* genes have not been verified.

Functional validation of wax synthesis genes *LbaFAR* and *LbaWSD1*

We constructed tobacco lines overexpressing the *LbaFAR* and *LbaWSD1* genes, labelled FAR-OE and WSD1-OE, respectively, measured their wax load and gene expression levels, and observed the wax coverage via SEM. The wax load in the wild type (WT) was 24.18 μg/cm^2, that in the FAR-OE line was 35.33 μg/cm^2, and that in the WSD1-OE line was 29.56 μg/cm^2, representing increases of 46.10% and 22.23%, respectively, compared with those in the WT($P < 0.05$) (Fig. 6A). The relative expression level of the *LbaFAR* gene in the WT and FAR-OE lines was 1.01 and 34.86, respectively ($P < 0.05$) (Fig. 6C). The relative expression level of the *LbaWSD1* gene in the WT line was 1.01, and that in WSD1-OE line was 50.74 ($P < 0.05$) (Fig. 6D). As shown in Fig. 6B, the leaves of the FAR-OE line significantly affected colour, lustre, and wax density, confirming the important role of the *LbaFAR* and *LbaWSD1* genes in wax synthesis.

Discussion

Wax load and leaf disease

Plant wax plays important roles in the interactions of plants with pathogenic and nonpathogenic

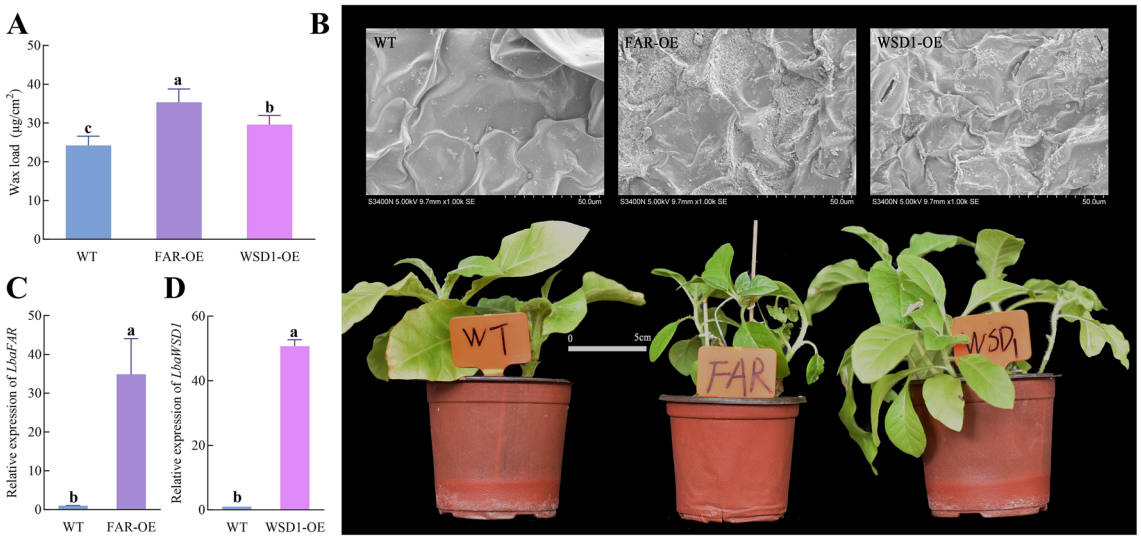

Fig. 6 Wax load, gene expression, and phenotypic in overexpression tobacco lines. **A** Wax load. **B** Images of phenotypic and SEM. **C** Relative expression level of *LbaFAR* gene in FAR-OE lines. **D** Relative expression level of *LbaWSD1* gene in WSD1-OE lines. Different letters on the column indicate significant differences, while the same letter indicates insignificant differences ($P < 0.05$)

microorganisms [21]. Wax serves not only as a physical barrier between plants and the environment but also as a source of signaling molecules for microbes and the host plant [6]. There are substantial differences in wax ultrastructure and composition among different plant species, organ types, and developmental stages [43, 44]. Previous studies have shown that the expression of the epicuticular pathogenesis-related protein-encoding gene *PR* in *CER2* and *CER6* deletion mutants of *A. thaliana* was significantly decreased [45]. The *Arabidopsis* cutin mutants *bdg*, *lacs2-3*, and *eca2* showed resistance to *Botrytis cinerea* [46]. Mutations in *SHINE* transcription factors related to *Arabidopsis* cuticle wax caused to defects in the stratum corneum and susceptibility to grey mould [12]. With the increase maturity of 'Navelate' citrus fruit, the cuticle became loose, cracks increased, wax was missing, and the fruit became very vulnerable to infection by *Penicillium digitatum* [9]. However, some studies have also shown that the wax load is negatively correlated with spore germination. For example, one study on bread wheat (*Triticum aestivum*) showed that knockout of *TaCHR729* led to the downregulation of *TaKCS6* transcription, reduced the accumulation of wax on leaves and decreased the germination of *Blumeria graminis* f.sp. *tritici* [14]; silencing the gene encoding enoyl-CoA reductase, which is a component of epicuticular wax biosynthesis, led to a reduction of in the epicuticular wax load and conidial germination of powdery mildew [47].

Most of the outer layer of the cuticle is formed by epicuticular waxes, which accumulate as an amorphous film or in microcrystalline structures [48]. The structure, thickness, and chemical composition of plant wax layers has major impacts on the occurrence of infectious diseases [8]. Terpenoids in goji berry wax can increase the resistance to decay caused by *A. alternata* [23]. Alkanes and triterpenoids found in the wax of apple pear peels can inhibit spore *A. alternata* germination and mycelial growth [49]. In this study, the wax load on the leaves of 'Ningqi I' goji plants was 3.36 times greater than that on the leaves of 'Huangguo' goji plants, and the distribution was uniform and dense. The content of alkane and alcohol were 24.87% and 121.18% greater, respectively, than those in 'Huangguo' goji. After 20 days of inoculation with powdery mildew, the disease index of 'Ningqi I' was 1.08, indicating HR. The disease index of 'Huangguo' goji was 24.49, indicating MS. There was a significant relationship between the wax load of goji leaves and disease resistance. After mechanical wax removal, the lesion area and disease index of the two varieties of goji plants increased significantly, indicating ES.

Relative expression of wax-coding genes and wax synthetase

Wax is metabolized in multiple organelles, and its synthesis, transport, and secretion involve a large number of enzymes and related genes [50]. Very long-chain fatty acids are precursors shared by wax synthesis pathways. The primary alcohols and wax esters synthesized by the alcohol-forming pathway constitute ~ 12% of leaf wax and 17% of stem wax on *A. thaliana*. Alkanes, aldehydes, secondary alcohols and ketones derived from the alkane-forming pathway account for > 80% of wax on *A. thaliana*

leaves and stems [51]. However, alcohols play a predominant role in leaf epicuticular wax in some important crops, such as corn and barley, where primary alcohols account for approximately 70–80% of the wax components [52, 53].

ACC, LACS, KCS and other enzymes are important for synthesizing very long chain fatty acids. FAR and WSD1 are important enzymes in the alcohol-forming pathway, while AD and MAH1 are important enzymes in the alkaline-forming pathway [6, 54]. In this study, KEGG and GO enrichment revealed that the expression levels of 17 DEGs related to wax synthesis in 'Ningqi I' were significantly greater than those in 'Huangguo' goji, which was consistent with the above results. According to the GC/MS results for the cuticular wax of leaves, there was a significant difference in the proportion of alcohols produced by the two goji varieties via the alcohol-forming pathway. We combined the activities of FAR and WSD1, and the relative expression levels of the *LbaFAR* and *LbaWSD1* genes and of *LbaFAR* and *LbaWSD1* were used for gene function validation.

Primary alcohols are assumed to be produced by the reduction of fatty acyl-CoA, catalyzed by FAR [55], which in turn acts as intermediate metabolites or metabolic end products to participate in the formation of plant extracellular lipid protective barriers [56]. *Atcer4* mutants exhibit major decreases in stem primary alcohols and wax esters, but the levels of alcohol-forming pathway components are slightly elevated [57]. *OsFAR1* encodes a fatty acyl-CoA reductase that is involved in the biosynthesis of primary alcohols and plays an important role in the drought stress response in rice [58]. WSD1 catalyses the formation of wax esters from primary alcohols and C16/C18 coenzyme A. *Arabidopsis* WSD1 catalyses the formation of wax esters using acyl-CoAs and primary alcohols as precursors in the alcohol-forming pathway [59]. After the WSD1 gene was knocked out, the total wax load of *Arabidopsis* mutant lines decreased by 15–20% [60]. Overexpression of *WSD1* could increase the leaf wax load of *A. thaliana* and *Camelina sativa*, ultimately enhancing osmotic stress tolerance [60]. The results of this study showed that the expression level of *LbaFAR* and the activity of FAR in 'Ningqi I' goji plants were significantly greater than those in 'Huangguo' goji plants, which was conducive to the production of more alcohols, as confirmed by the GC/MS and FAR-OE results for the tobacco lines. The expression level of *LbaWSD1* was relatively high in 'Ningqi I' goji, but the WSD1 activity and the ester contents were not significantly different from those in 'Huangguo' goji. The expression level of *LbaWSD1* was high in WSD1-OE tobacco lines, but the increase in wax load was relatively small, which may be due to differences in wax ester synthesis among the different varieties; alternatively, WSD1, as the end of wax ester synthesis, has high activity but lacks synthetic precursors.

Disease resistance application prospects of goji leaf wax

Powdery mildew is one of the main leaf diseases of goji plants and rapidly spreads throughout main production areas, such as Gansu, Ningxia, and Qinghai Province. It mainly harms new shoots and leaves, seriously affecting leaf photosynthesis, and thereby reducing fruit yield and quality and even causing crop failure [17, 19]. An investigation in September 2014 revealed that ~ 70% of the goji fields around Wuzhong city were affected by powdery mildew [18]. At present, the control of goji powdery mildew mainly relies on agricultural chemicals, leading to excessive residue accumulation in fruits [21]. According to statistics on the field incidence rate and disease index of powdery mildew in sixteen goji varieties, 'Ningqi I' goji is highly resistant to powdery mildew, and 'Huangguo' goji exhibits the opposite trend [19]. This study showed that the incidence rate and disease index of 'Huangguo' goji after artificial inoculation of powdery mildew were significantly greater than those of 'Ningqi I', with MS to powdery mildew infection. The incidence rate and disease index of 'Ningqi I' showed an HR for powdery mildew infection.

In this study, we planned to inoculate the goji powdery mildew pathogen into the FAR-OE and WSD1-OE lines, but due to differences in host range, this process was not successful. In future research, homologous transformation of *LbaFAR* and *LbaWSD1* will be performed, and then, powdery mildew will be inoculated to further confirm the relationship between the wax synthesis gene and resistance to powdery mildew.

In summary, differences in wax load, crystal morphology and composition contribute to differences in the colour and lustre of goji leaves. Through transcriptomic data mining, the differential wax load in the leaves of the two varieties may be attributed to important genes involved in fatty acid synthesis (*LbaACC, LbaLACS,* and *LbaKCS*) and wax biosynthesis (*LbaFAR, LbaWSD1,* and *LbaMAH1*). The relative expression of six coding genes and enzyme activities were assessed, in conjunction with the findings from GC/MS analysis as well as KEGG and GO enrichment analyses. The results collectively suggest that *LbaFAR* and *LbaWSD1* are involved in the alcohol-forming pathway and are pivotal factors influencing the load and composition of wax. After the two genes were transferred to tobacco, the relative expression levels and leaf wax loads of FAR-OE and WSD1-OE lines significantly increased, but the degree of improvement varied. The incidence rate and disease index of 'Ningqi I' goji were significantly lower

than those of 'Huangguo' goji when the goji powdery mildew pathogen was inoculated on the leaves. The high expression of the *LbaFAR* and *LbaWSD1* genes led to an increase in FAR and WSD1 activity in 'Ningqi I' leaves, and the wax load and alcohol content in the leaf epidermis of goji plants increased, resulting in glossiness, thereby increasing resistance to goji powdery mildew. Furthermore, these research results can provide a theoretical basis for the production of low agricultural chemical residue goji and the breeding of powdery mildew resistant varieties.

Abbreviations

UV	Ultraviolet
SEM	Scanning electron microscopy
RT–qPCR	Real time quantitative polymerase chain reaction
ELISA	Enzyme-linked immunosorbent assay
FAA	Formaldehyde-acetic acid–ethanol
GC/MS	Gas chromatography–mass spectrometry
FID	Flame ionization detector
RNA	Ribonucleic acid
GO	Gene ontology
KEGG	Kyoto encyclopedia of genes and genomes
PBS	Phosphate buffered saline
ACC	Acetyl CoA carboxylase
LACS	Long chain acyl-CoA synthase
KCS	β-Ketoacyl CoA synthase
FAR	Fatty acyl reductases
WSD1	Wax ester synthase
MAH1	Medium chain alkane hydroxylase
LB	Luria bertani
OD	Optical density
PCA	Principal components analysis
DEGs	Differentially expressed genes
HR	High resistance
MS	Moderate susceptibility
ES	Extreme susceptibility

Supplementary Information

The online version contains supplementary material available at https://doi.org/10.1186/s40538-024-00590-0.

Additional file 1: Table S1. The primers of RT- qPCR expression analysis. **Table S2.** Gene clone primers. **Table S3.** Double enzyme cleavage primers. **Table S4.** Classification criteria for the incidence of powdery mildew on goji leaves. **Table S5.** Evaluation criteria for resistance of goji leaves to powdery mildew. **Table S6.** Quality detection of transcriptome data from 'Ningqi I' and 'Huangguo' goji. **Figure S1.** The PCA and volcano plot of 'Ningqi I 'between 'Huangguo 'goji. Note: A PCA of transcriptome sequencing data, B Volcano plot of DEGs. H Abbreviation for 'Huangguo' goji, N Abbreviation for 'Ningqi I 'goji. **Figure S2.** GO enrichment analysis of DEGs. **Figure S3.** KEGG enrichment analysis of DEGs

Acknowledgements
We thank for Professor Zhongjian Liu from Fujian A&F University shared the reference genome.

Author contributions
JL was mainly responsible for project management and wrote the manuscript, XW was a major contributor to data analysis, SDZ was conducted enzyme assay, XZ conducted the RT–qPCR experiments, XZ and LDF performed the assays of tobacco lines, JH designed this research. All authors read, commented on and approved the final manuscript.

Funding
This study was supported by the National Natural Science Foundation of China: 32060341.

Availability of data and materials
Not applicable.

Declarations

Ethics approval and consent to participate
Not applicable.

Consent for publication
Not applicable.

Competing interests
The authors declare that they have no competing interests.

Author details
[1]College of Forestry, Gansu Agricultural University, Lanzhou, China. [2]Wolfberry Harmless Cultivation Engineering Research Center of Gansu Province, Lanzhou, China. [3]Industry Development and Planning Institute, National Forestry and Grassland Administration, Beijing, China. [4]College of Food Science and Engineering, Gansu Agricultural University, Lanzhou, China.

Received: 5 February 2024 Accepted: 24 April 2024
Published online: 29 April 2024

References

1. Riederer M. Biology of the plant cuticle. Ann Plant Rev. 2007;23:1–10.
2. Cheng GP, Huang H, Zhou LY, He SG, Zhang YJ, Cheng XA. Chemical composition and water permeability of the cuticular wax barrier in rose leaf and petal: a comparative investigation. Plant Physiol Biochem. 2019;135:404–10.
3. Xue DW, Zhang XQ, Lu XL, Chen G, Chen ZH. Molecular and evolutionary mechanisms of cuticular wax for plant drought tolerance. Front Plant Sci. 2017;8:621.
4. Khanal BP, Grimm E, Finger S, Blume A, Knoche M. Intracuticular wax fixes and restricts strain in leaf and fruit cuticles. New Phytol. 2013;200(1):134–43.
5. Buschhaus C, Jetter R. Composition and physiological function of the wax layers coating Arabidopsis leaves: beta-amyrin negatively affects the intracuticular water barrier. Plant physiol. 2012;160(2):1120–9.
6. Lewandowska M, Keyl A, Feussner I. Wax biosynthesis upon danger: its regulation upon abiotic and biotic stress. New Phytol. 2020;227:698.
7. Nishiyama T, Sakayama H, De Vries J, Buschmann H, Saint-Marcoux D, Ullrich KK, et al. The chara genome: secondary complexity and implications for plant terrestrialization. Cell. 2018;174(2):448–64.
8. Konarska A. Differences in the fruit peel structures between two apple cultivars during storage. Agric Food Sci. 2012;11:105–16.
9. Cajuste JF, González-Candelas L, Veyrat A, García-Breijo FJ, Reig-Armiñana J, Lafuente MT. Epicuticular wax content and morphology as related to ethylene and storage performance of 'Navelate' orange fruit. Postharvest Biol Tec. 2010;55(1):29–35.
10. Fahlberg P, Buhot N, Johansson ON, Andersson MX. Involvement of lipid transfer proteins in resistance against a non-host powdery mildew in *Arabidopsis thaliana*. Mol Plant Pathol. 2019;20(1):69–77.
11. Reisberg EE, Hildebrandt U, Riederer M, Hentschel U. Distinct phyllosphere bacterial communities on *Arabidopsis* wax mutant leaves. PLoS ONE. 2013;8(11): e78613.
12. Sela D, Buxdorf K, Shi JX, Feldmesser E, Schreiber L, Aharoni A, et al. Overexpression of *AtSHN1/WIN1* provokes unique defense responses. PLoS ONE. 2013;8(7): e70146.
13. Castorina G, Bigelow M, Hattery T, Zilio M, Sangiorgio S, Caporali E, et al. Roles of the *MYB94/FUSED LEAVES1* (*ZmFDL1*) and *GLOSSY2* (*ZmGL2*)

genes in cuticle biosynthesis and potential impacts on *Fusarium verticillioides* growth on maize silks. Front Plant Sci. 2023;14:1228394.
14. Xiong WD, Liao LX, Ni Y, Gao HC, Yang JF, Guo YJ. The effects of epicuticular wax on anthracnose resistance of sorghum bicolor. Int J Mol Sci. 2023;24(4):3070.
15. Amagase H, Farnsworth NR. A review of botanical characteristics, phytochemistry, clinical relevance in efficacy and safety of *Lycium barbarum* fruit (Goji). Food Res Int. 2011;44(7):1702–17.
16. Shah T, Bule M, Niaz K. Goji berry (*Lycium barbarum*)—a superfood. In: Nabavi SM, Silva AS, editors. Nonvitamin and nonmineral nutritional supplements. USA: Academic Press; 2019. p. 257–64.
17. Qin K, Yang J, Liu J, Ma Z. Preliminary discussion on the organic prevention and control of powdery mildew of *Lycium barbarum* L. Northern Hortic. 2016;16:110–2 (**in Chinese**).
18. Wang RY, Zhao X, Hao HT, Shang QH, Yang G. First report of *Arthrocladiella mougeotii* causing powdery mildew on goji berry (*Lycium barbarum*) in Ningxia, China. Plant Dis. 2015;99(9):1283.
19. Li Y, Nie F, Li Y. Investigation on powdery mildew resistance of different wolfberry cultivars. Ningxia Agric Forestry Tech. 2023;64(01):16–9 (**in Chinese**).
20. Qin K, Duan L, Yang J, Huang T. Comparative study on control effects of three kinds of sulfur preparations against wolfberry powdery mildew. Ningxia Agric Forestry Tech. 2018;59(6):15–6 (**in Chinese**).
21. Ding L, Zhou X, Liang XJ, Dong YJ, Fang CB, Wu YM, et al. Achieving high efficacy and low safety risk by balancing pesticide deposition on leaves and fruits of Chinese wolfberry (*Lycium barbarum* L.). ACS Omega. 2023;8(16):14672–83.
22. Sun Q, Du M, Kang Y, Zhu MJ. Prebiotic effects of goji berry in protection against inflammatory bowel disease. Crit Rev Food Sci Nutr. 2023;63(21):5206–30.
23. Wang P, Wang J, Zhang H, Wang C, Zhao L, Huang T, et al. Chemical composition, crystal morphology, and key gene expression of the cuticular waxes of goji (*Lycium barbarum* L.) berries. J Agric Food Chem. 2021;69(28):7874–83.
24. Li J, Feng L, Li D, Liu X, Pan Y, He J, et al. ROS regulate NCF2, key metabolic enzymes and MDA levels to affect the growth of *Fusarium solani*. Agriculture. 2022;12(11):1840.
25. Hu J, Liu Y, Tang X, Rao H, Ren C, Chen J, et al. Transcriptome profiling of the flowering transition in saffron (*Crocus sativus* L.). Sci Rep. 2020;10(1):9680.
26. Wang Y, Zeng J, Xia X, Xu Y, Chen S. Comparative analysis of leaf trichomes, epidermal wax and defense enzymes activities in response to *Puccinia horiana* in chrysanthemum and *Ajania* species. Hortic Plant J. 2020;6(3):8.
27. Chu W, Gao H, Cao S, Fang X, Chen H, Xiao S. Composition and morphology of cuticular wax in blueberry (*Vaccinium* spp.) fruits. Food Chem. 2017;219:436–42.
28. Yang Z, Xiaojuan L, Mengke W, Quanxin B, Yifan C, Libing W. Transcriptome and physiological analyses provide insights into the leaf epicuticular wax accumulation mechanism in yellowhorn. Hortic Res. 2021;8(1):134.
29. Li N, Song Y, Li J, Hao R, Feng X, Li L. Transcriptome and genome re-sequencing analysis reveals differential expression patterns and sequence variation in pericarp wax metabolism-related genes in *Ziziphus jujuba* (Chinese jujube). Sci Hortic. 2021;288: 110415.
30. Tian L, Shang S, Yang Y, Si L, Li D. Relationship between the leaf structure of bitter melon and resistance to powdery mildew. Acta Botan Boreali-Occiden Sin. 2013;33(10):2010–5 (**in Chinese**).
31. Jing X, Wang H, Gong B, Liu S, Wei M, Ai X, et al. Secondary and sucrose metabolism regulated by different light quality combinations involved in melon tolerance to powdery mildew. Plant Physiol Biochem. 2018;124:77–87.
32. Figueiredo K, Oliveira M, Oliveira AF, Silva G, Santos M. Epicuticular-wax removal influences gas exchange and water relations in the leaves of an exotic and native species from a Brazilian semiarid region under induced drought stress. Aust J Bot. 2012;60:685.
33. Kim D, Langmead B, Salzberg SL. HISAT: a fast spliced aligner with low memory requirements. Nat Methods. 2015;12(4):357–60.
34. Roberts A, Trapnell C, Donaghey J, Rinn JL, Pachter L. Improving RNA-Seq expression estimates by correcting for fragment bias. Genome Biol. 2011;12(3):1–14.
35. Anders S, Theodor P, Huber W. HTSeq—a Python framework to work with high-throughput sequencing data. Bioinformatics. 2015;31(2):4.
36. Love MI, Huber W, Anders S. Moderated estimation of fold change and dispersion for RNA-seq data with DESeq2. Genome Biol. 2014;15(12):550.
37. Albou LP. The gene ontology resource: 20 years and still GOing strong. Nucleic Acids Res. 2019;47:9.
38. Kanehisa M, Araki M, Goto S, Hattori M, Itoh M. KEGG for linking genomes to life and the environment. Nucleic Acids Res. 2008;36(Suppl 1):D480–4.
39. Livak KJ, Schmittgen TD. Analysis of relative gene expression data using real-time quantitative PCR. Methods. 2002;25(4):402–8.
40. Tao YX, Peer AFV, Huang QH, Shao YP, Xie BG. Identification of novel and robust internal control genes from *Volvariella volvacea* that are suitable for RT-qPCR in filamentous fungi. Sci Rep. 2016;6:29236.
41. Jeffree CE. The fine structure of the plant cuticle. UK: Blackwell Publishing Ltd; 2006. p. 11–125.
42. Li-Beisson Y, Shorrosh B, Beisson F, Andersson MX, Arondel V, Bates PD, et al. Acyl-lipid metabolism. The Arabidopsis Book. 2013; 11:161.
43. Buda GJ, Barnes WJ, Fich EA, Park S, Yeats TH, Zhao L, et al. An ATP binding cassette transporter is required for cuticular wax deposition and desiccation tolerance in the moss *Physcomitrella patens*. Plant Cell. 2013;25(10):4000–13.
44. Renault H, Alber A, Horst NA, Basilio Lopes A, Fich EA, Kriegshauser L, et al. A phenol-enriched cuticle is ancestral to lignin evolution in land plants. Nat Commun. 2017;8(1):14713.
45. Garbay B, Tautu MT, Costaglioli P. Low level of pathogenesis-related protein 1 mRNA expression in 15-day-old *Arabidopsis cer6-2* and *cer2* eceriferum mutants. Plant Sci. 2006;172(2):299–305.
46. Aragón W, Formey D, Aviles-Baltazar NY, Torres M, Serrano M. *Arabidopsis thaliana* cuticle composition contributes to differential defense response to *Botrytis cinerea*. Front Plant Sci. 2021;12:1.
47. Kong L, Zhi P, Liu J, Li H, Zhang X, Xu J, et al. Epigenetic activation of enoyl-CoA reductase by an acetyltransferase complex triggers wheat wax biosynthesis1. Plant Physiol. 2020;183(3):1250–67.
48. Barthlott W, Neinhuis C, Cutler D, Ditsch F, Meusel I, Theisen I, et al. Classification and terminology of plant epicuticular wax. Bot J Linn Soc. 2008;126:237–60.
49. Yin Y, Bi Y, Chen S, Li Y, Wang Y, Ge Y, et al. Chemical composition and antifungal activity of cuticular wax isolated from Asian pear fruit (cv. Pingguoli). Sci Hortic. 2011;129(4):577–82.
50. Lara I, Belge B, Goulao LF. The fruit cuticle as a modulator of postharvest quality. Postharvest Biol Tec. 2014;87:103–12.
51. Bernard A, Joubès J. *Arabidopsis* cuticular waxes: advances in synthesis, export and regulation. Prog Lipid Res. 2013;52(1):110–29.
52. Hasanuzzaman M, Davies NW, Shabala L, Zhou M, Brodribb TJ, Shabala S. Residual transpiration as a component of salinity stress tolerance mechanism: a case study for barley. BMC Plant Biol. 2017;17(1):107.
53. Javelle M, Vernoud V, Depège-Fargeix N, Arnould C, Oursel D, Domergue F, et al. Overexpression of the epidermis-specific homeodomain-leucine zipper IV transcription factor outer cell layer1 in maize identifies target genes involved in lipid metabolism and cuticle biosynthesis. Plant Physiol. 2010;154(1):273–86.
54. Lim GH, Singhal R, Kachroo A, Kachroo P. Fatty acid- and lipid-mediated signaling in plant defense. Annu Rev Phytopathol. 2017;55:505–36.
55. Huang L, Xiao Q, Zhao X, Wang D, Wei L, Li X, et al. Responses of cuticular waxes of faba bean to light wavelengths and selection of candidate genes for cuticular wax biosynthesis. Plant Genome. 2020;13(3): e20058.
56. Zhang X, Liu Y, Ayaz A, Zhao H, Lü S. The plant fatty acyl reductases. Int J Mol Sci. 2022;23(24):16156.
57. Rowland O, Zheng H, Hepworth SR, Lam P, Jetter R, Kunst L. *CER4* encodes an alcohol-forming fatty acyl-coenzyme A reductase involved in cuticular wax production in *Arabidopsis*. Plant physiol. 2006;142(3):866–77.
58. Guan L, Xia D, Hu N, Zhang H, Wu H, Jiang Q, et al. *OsFAR1* is involved in primary fatty alcohol biosynthesis and promotes drought tolerance in rice. Planta. 2023;258(2):24.

59. Li F, Wu X, Lam P, Bird D, Zheng H, Samuels L, et al. Identification of the wax ester synthase/acyl-coenzyme A:diacylglycerol acyltransferase WSD1 required for stem wax ester biosynthesis in *Arabidopsis*. Plant Physiol. 2008;148(1):97–107.
60. Abdullah HM, Rodriguez J, Salacup JM, Castañeda IS, Schnell DJ, Pareek A, et al. Increased cuticle waxes by overexpression of *WSD1* improves osmotic stress tolerance in *Arabidopsis thaliana* and *Camelina sativa*. Int J Mol Sci. 2021;22(10):5173.

Publisher's Note